17th Int. Conf. on Acc. and Large Exp. Physics Control Systems ICALEPCS2019, New York, NY, USA JACoW Publishing
ISBN: 978-3-95450-209-7 ISSN: 2226-0358 doi:10.18429/JACoW-ICALEPCS2019-MOCPL06

2D-NANO-PTYCHOGRAPHY IMAGING RESULTS ON THE SWING BEAMLINE AT SYNCHROTRON SOLEIL

C. Engblom*, Y-M. Abiven, F. Alves, F. Berenguer, T. Bizien,
A. Gibert, F. Langlois, A. Lestrade, P. Montaville, J. Pérez
Synchrotron SOLEIL, St Aubin, France

Abstract

A new Nanoprobe system, which was originally developed in the scope of a collaboration with MAXIV (Sweden), has recently been tested and validated on the SWING beamline in Synchrotron SOLEIL. The aim of the project was to construct a Ptychography nano-imaging station. Initial steps were taken to provide a portable system capable of nanometric scans of samples with sizes ranging from the micrometer to fractions of a millimeter. Imaging was made possible by actuating a total of 16 Degrees Of Freedom (DOF) composed of a sample stage (3 DOF), a central stop stage (5 DOF), a Fresnel zone plate stage (5 DOF), as well as an order sorting aperture stage (3 DOF). These stages were actuated by an ensemble of piezo-driven and high-quality brushless motors, of which synchronized control (with kinematic modelling) was done using the Delta Tau platform. In addition, interferometry feedback was used for reconstruction purposes. Imaging results are promising: the system was able to resolve 40 nm measured with a Siemens star, the paper will describe the system and the achieved results.

INTRODUCTION

The *Nanoprobe Project* [1] was a 4-year joint collaboration between Synchrotron SOLEIL and MAXIV (Sweden), where a 3D scanning-nanoprobe prototype was produced. This project officially ended in december 2016 - after which a SOLEIL-based team dedicated to nano-positioning systems was formed (*Nanoprobe-SOLEIL*).

In part inspired by the cSAXS beamline (Swiss Light Source), the SWING beamline [2] at Synchrotron SOLEIL has decided to add high-resolution coherent diffractive imaging, ptychography, to its roster of experimental setups. The reason for this is two-fold; first to address a growing need amongst its users, and secondly to prepare for the upcoming SOLEIL synchrotron upgrade [3] which will utilize a more coherent light source. High-resolution imaging is the driving factor here - the overall aim is to achieve the *nanometer* scale of 20 nm (or better) over full-range sample scans of 10 µm up to several 100 µm. Another major constraint is system portability; to keep a level of flexibility between different type of experiments, any new system needs to be compact and capable of installing/uninstalling to/from the beamline within a few hours.

The scope of the project (and the subject of this paper) is therefore to: install a Nanoprobe system on the SWING beamline, and have it tested & validated through 2D nano-

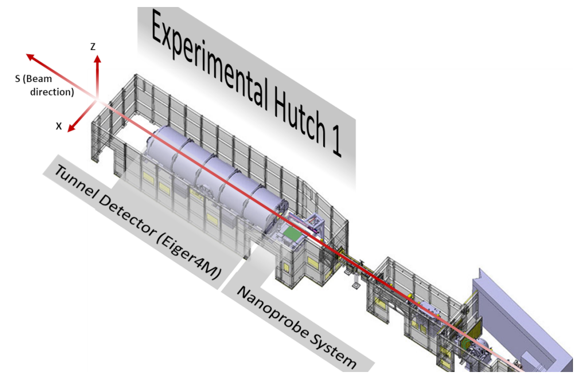

Figure 1: Overview of the SWING experimental hutch 1 (EH1), here marked out with the SOLEIL SXZ- orientation; the location of the Eiger 4M detector has been pointed out (inside a 7 meters long in-vacuum tunnel), as well as the location of the Nanoprobe System.

ptychography imaging. The *Nanoprobe Project* [1] will be used as an outline for the new SWING setup, where the previously produced prototype will be re-used & adapted to beamline specifications. As such, we will rely heavily on:

1. Support structure & system environment; rigidity and thermal stabilization via enclosure of some kind.
2. High- resolution (capable of resolving a nanometer), long-range (several millimetres) positioners.
3. Interferometry; a tool to qualify and measure motion errors - to either be used for correcting images post-process, or be implemented in closed-loop control.
4. Control Systems; for high-frequency control, & multi-axis synchronization via kinematic modeling if need be.

Figure 1 shows an overview of the EH1 experimental hutch where the Nanoprobe System will be installed and tested.

The term *Nanoprobe End-Station* will in this paper be referred to the support and environment that houses the active parts used in scans. The term *Nanoprobe System* will refer to the Nanoprobe End-Station *as well as* all its driving electronics & control systems.

NANOPROBE END-STATION OVERVIEW

The end-station can be divided up into five primary parts, four *stages* and their support structure. Figure 2 illustrates

* christer.engblom@synchrotron-soleil.fr

ISBN: 978-3-95450-209-7 ISSN: 2226-0358 doi:10.18429/JACoW-ICALEPCS2019-MOCPL06

the setup, showing each stage and their respective Degrees-of-Freedom (DOF).

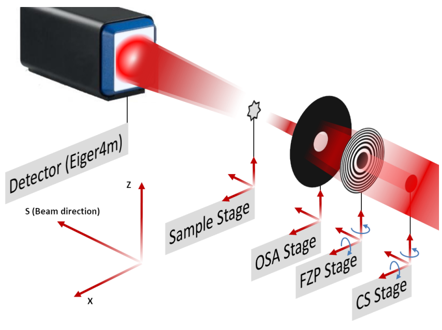

Figure 2: Principal scheme outlining the SXZ- orientation of the Nanoprobe End-Station stages and their respective degrees of freedom.

Support & Environment

The EH1 hutch environment stability was ensured by performing vibrational analysis prior to installation. A one-piece aluminium support for the stages was constructed (see Fig. 3); some compromises were made in the conception of the support structure in order adhere to beamline specifications.

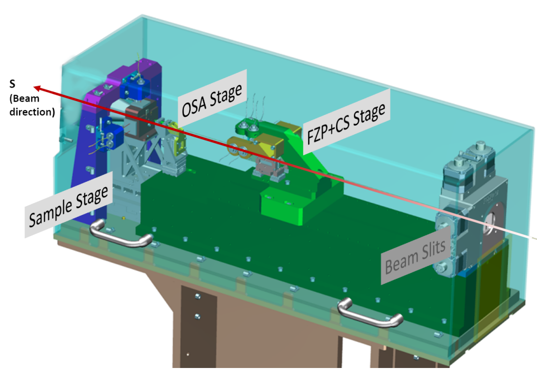

Figure 3: Nanoprobe stage support & environment. A plexiglass cover was added for thermal stabilisation and to minimize air turbulence.

FZP & CS Stages

These stages, see Fig. 4, were originally designed to hold two Fresnel-Zone plates (FZP) actuating into 5 DOF. In the scope of the SWING implementation, they were adapted to instead hold one FZP and one Central-Stop (CS) plate, but still maintaining the same amount of DOF as before. These stages were identical and symmetric modules that each held their respective optical elements in cradles. Both stages actuated into five DOF; linear translations in the SXZ-space and two DOF in the Rs and Rz space. The primary objective of these stages was, besides positioning, holding stability over the duration of the scans - this means that any error drifts (from thermal dilations or otherwise) would be minimized or corrected for. All positional drives were of piezo stick-and-slip types, allowing for high-resolution (1 nm) and long travel ranges (mm- range). In addition, both stages were equipped with interferometry sensors to provide (X, Z, Rx, Rz)- feedback for closed-loop control - more on this in Section *Control & Acquisition*.

Note that these stages , but having been

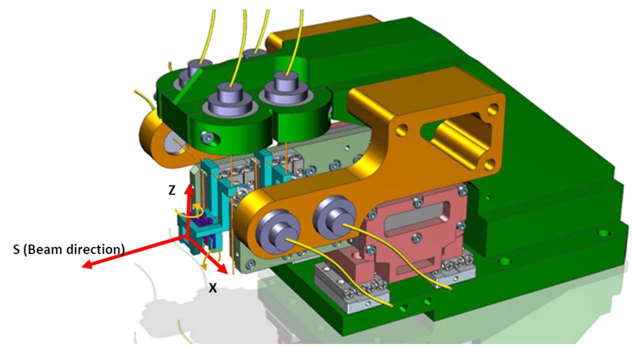

Figure 4: 3D model of the Fresnel-Zone-Plate (FZP) Stage, and Central-Stop (CS) Stage with 8 interferometer sensor heads. Annotated (red and orange arrows) DOF (X, S, Z, Rx, Rz) on the Fresnel Zone Plate.)

OSA Stage

This stage was actuated by three stacked encoded linear piezo-multi-leg positioners, allowing for high-resolution (0.5 nm) and long-range movements in the millimetre range. The stage actuated into three linear DOF in the SXZ- space (see Fig. 5).

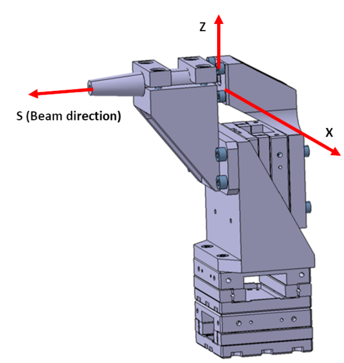

Figure 5: 3D model of Order-Sorting-Aperture (OSA) Stage, here annotated with its three DOF.

Sample Stage

The sample stage consisted of three stacked linear and encoded positioners that actuated into three DOF over the SXZ- space. 2D-ptychography scans would involve small incremental steps on the XZ- plane while the S-positioner would hold its position; these 2D-scans would normally be in deca- or hundreds of nanometer step increments over a span of deca-micrometers. Figure 6 shows the setup of the sample stage, here with an overlying bracket holding interferometer sensors for sample tracking during scans. Interferometer

ISBN: 978-3-95450-209-7 ISSN: 2226-0358 doi:10.18429/JACoW-ICALEPCS2019-MOCPL06

measurements would only be used for tracking movement errors for post-process image corrections.

The X- positional drive was of high-precision brushless motor, while the SZ- positioners were of piezo multi-leg types. These drives all allowed for high-resolution steps (1 nm) over a range of > 10 mm.

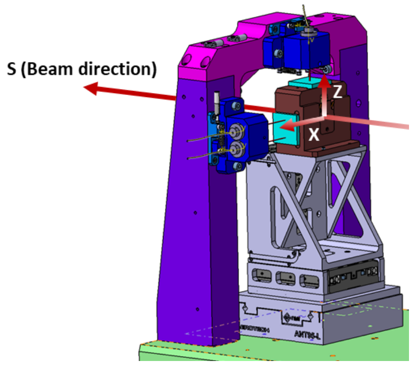

Figure 6: 3D model of the Sample Stage, here annotated with its three DOF. Also shown, a rigid bracket (marked blue) holding interferometry sensors towards the Sample stage, thus providing (X, Z, Rs) - feedback on the Sample stage at sample level.

CONTROL & ACQUISITION

System Architecture

Figure 7 shows the control architecture where user control is applied by interfacing to the driver electronics via a 4-controller Delta Tau PowerPMAC system setup (Soleil high-end controller from the REVOLUTION project [4, 5]). One controller was dedicated for the sample stage, while three interlinked controllers (Delta Tau MACRO interface [6]) were used for positional control & stability of the optical elements in the FZP, CS, & OSA stages. Control of the FZP/CS stages necessitated three interlinked controllers to maintain synchronized control (using kinematic models) of its 10 positional drives with full access to the 8 interferometer feedback sources.

The TANGO control system [7] is here used at user-level, interfacing directly with the Delta Tau controllers and interferometer readings for controls as well as data acquisition.

Control Schemes

System control strategies can be divided up into:

- Sample/OSA Stages (See Fig. 8): since these stages are of a stacked SXZ- design, control-loops can be applied individually & separately to each axis - here implemented as a high-frequency PID regulation.
- FZP/CS Stages (see Fig. 9): their stacked/parallel design not only necessitates multi-axial synchronization, but does so by using kinematic models - this allows for moving the rotational axes to the centre of the optical elements. A key step in this implementation is that interferometry feedback can be used for long-term holding stability - this to minimize motion errors such as thermal drifts.

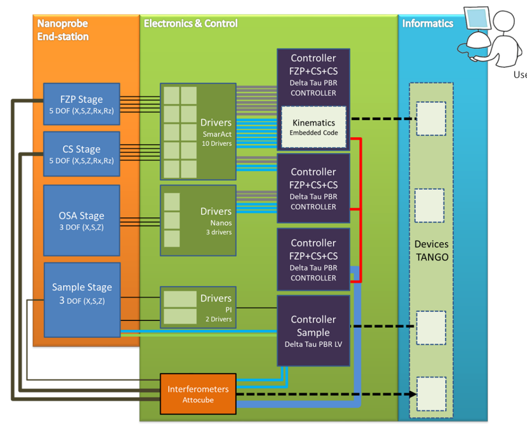

Figure 7: Control/Acquisition architecture, from/to the Nanoprobe end-station to/from the users via the electronics and high-level software (TANGO).

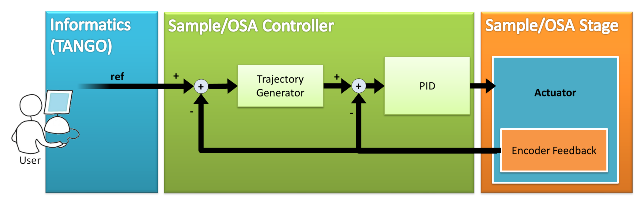

Figure 8: Sample/OSA control scheme, high-frequency standard PID regulation with the positional drive encoder as feedback.

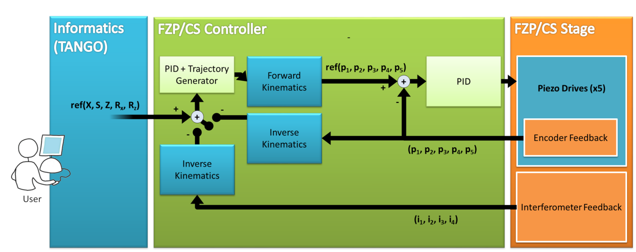

Figure 9: FZP/CS control scheme, multi-axial cascade-loop where the innermost loop is a high-frequency standard PID regulation with the drive encoder as feedback. The outermost loop calculates the five trajectories for each positioner in function of the virtual axes (X,S,Z,Rx,Rz)

STAGE EVALUATIONS

Before beamline installation, the different stages were assessed for motion errors in the scope of their respective uses; meaning long-term (≈20 min up to several hours) positioning stability of the optical stages & 2D-scanning performance of the sample stage. Note that the evaluations concerning the FZP- & OSA stages have been left out; the OSA sta-

ISBN: 978-3-95450-209-7 ISSN: 2226-0358 doi:10.18429/JACoW-ICALEPCS2019-MOCPL06

bility constraints weren't particularly high, and the FZP is considered a duplicate of the CS stage.

CS Stage

Two additional mirrors were glued to the optical cradle on the CS stage - each mirror setting up additional interferometers for assessments along the XZ- axes. Tests on the CS stage essentially illustrates two approaches for long-term positioning stability:

1. *System ON/OFF* (Fig. 10): error drifts (400 nm/h) along the Z-axes are evident when positioners are set to ON (closed-loop using encoder feedback). The drift-rate is however slowed down (25 nm/h) when the positioners are set to OFF. In addition, peak-to-peak vibrations (ON $\approx \pm 10$ nm, OFF $\approx \pm 5$ nm) are also clearly diminished.

2. *Interferometer Closed-loop ON/OFF* (Fig. 11): error drifts (100 nm/h) along the X-axes are evident when positioners are set to ON (closed-loop using encoder feedback). The moment interferometer closed-loop control is activated, this drift diminishes (2.5 nm/h), but peak-to-peak vibrations increase by a factor of two (Interferometers Closed-loop OFF, $\approx \pm 10$ nm, Interferometers Closed-loop ON, $\approx \pm 20$ nm).

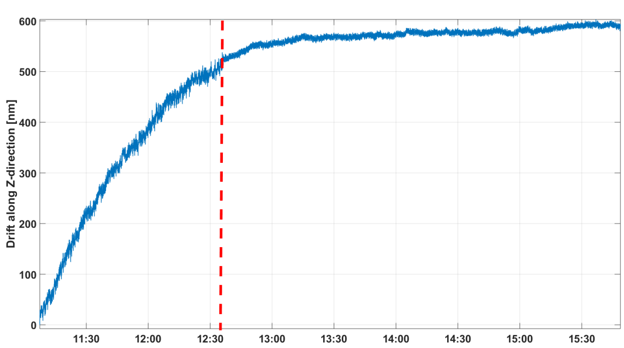

Figure 10: Central Stop Z-error drifts (over $\approx$5 h), thermal drifts in response to system ON/OFF. All positional drives were set to ON (closed-loop regulation with encoders) at start. The red dashed line indicates a moment in which all positional drives were set to OFF. No interferometer closed-loop was used in this test.

Sample Stage

The sample stage motion errors were measured using the interferometer bracket (see Fig. 6), from having executed a series of 2D-scans along the XZ- plane. Figure 12 shows motion errors from these scans, originating from the X-actuation (blue), or from the Z-actuation (red). Overall, motion errors in the both X- & Z- directions lies within a band of ± 100 nm.

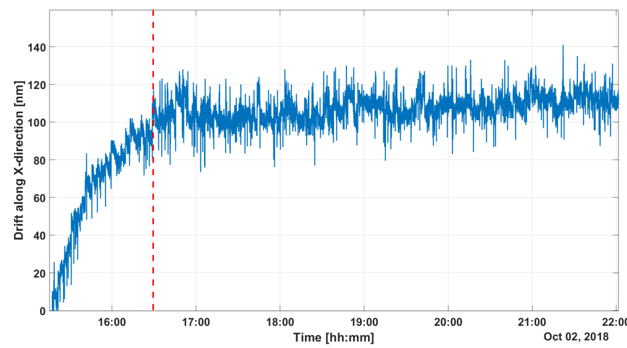

Figure 11: Central Stop X-error drifts (over $\approx$5 h), thermal drifts in response to interferometer closed-loop ON/OFF. All positional drives were set to ON (closed-loop regulation with encoders) at start. The red dashed line indicates a moment in which interferometer closed-loop was activated (as seen in Fig. 9).

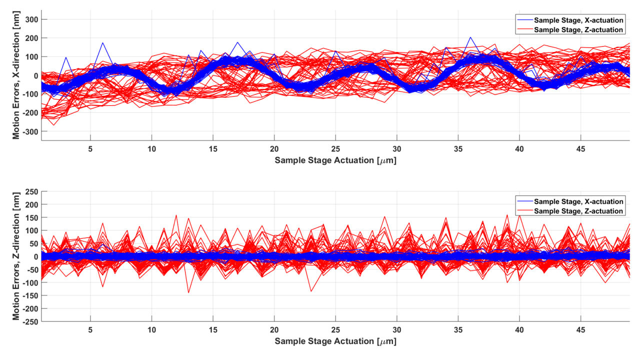

Figure 12: Sample Stage motion errors (along X- & Z-directions) that originates from of X-actuation (blue) or Z-actuation (red). Despite using high-quality and high-resolution positional drives, error motions in the magnitude of ± 100 nm are evident.

RESULTS

System Installation

Figure 13 shows the full Nanoprobe End-Station including the electronic bay installed in the EH1 experimental hutch, as well as the Nanoprobe end-station on a rolling cart, having just been unistalled fom the beamline. All in all, it took roughly three hours to uninstall the system from the beamline.

2D-Imaging Results

Figures 14 and 15 shows reconstructed phase images of the 50-nm Siemens star sample. Figure 14 gives the full overview of the scan - here the outer-most spokes (marked by the red box) resolves 0.5 μm; Fig. 15 shows the same image but focused on the centre of the sample, where one can visually resolve the innermost 50 nm spokes.

The system resolution is assessed by image comparisons from two different scans (and thus finding image repeatability) using the Fourier Shell Reconstruction (FSC) method [8]

ISBN: 978-3-95450-209-7 ISSN: 2226-0358 doi:10.18429/JACoW-ICALEPCS2019-MOCPL06

Figure 13: Left: The Nanoprobe system installed in EH1 (End-station & Electronic Bay). Right: The Nanoprobe end-station uninstalled and in transport (Left to right: C. Engblom, F. Alves, J. Perez).

Fig. 16 shows the correlation factor using the FSC 1 bit cutoff criteria - here we can see that the system repeatability (and in a way, system resolution) is calculated to be at 40.89 nm.

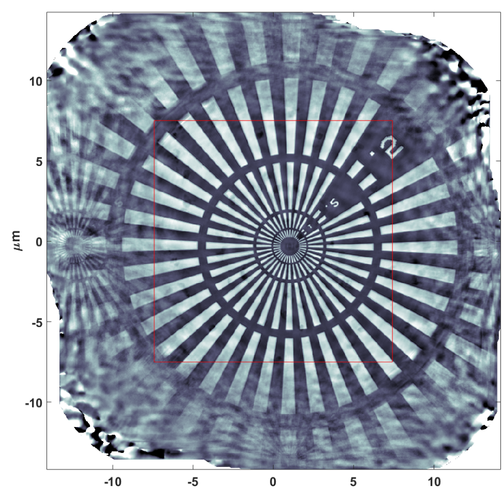

Figure 14: The reconstructed phase image of the Siemens Star; here given full overview up until the 0.5 μm stripes. As is expected, imaging artifacts can be found at the borders. Note that the spoke-size annotation is mirror inverted (due to sample placement during scan).

SUMMARY & CONCLUSION

A Nanoprobe system was constructed, installed, & ultimately tested by performing 2D-nano-ptychography imaging at the SWING beamline - where the imaging resolution was confirmed to be at 40nm (see Fig. 16). In addition, the system could be installed or uninstalled from/to the beamline within a few hours (see Fig. 13).

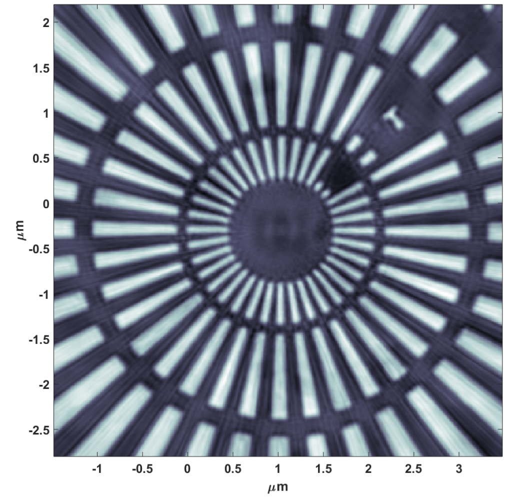

Figure 15: The reconstructed phase image of the Siemens Star; here focused on the centre of the sample - fully resolving the 50 nm spokes of the Siemens Star. Note that the spoke-size annotation is mirror inverted (due to sample placement during scan).

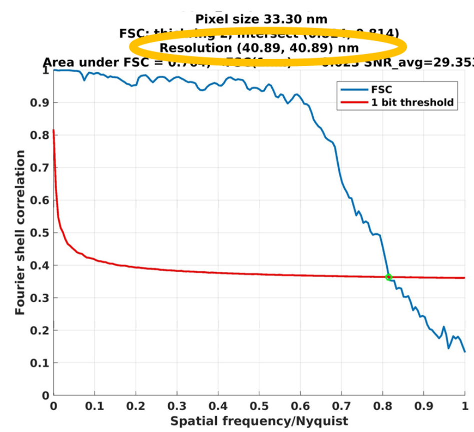

Figure 16: System resolution (or image repeatability) is estimated by two-image comparisons using Fourier Shell Correlation with an FSC 1-bit cutoff criteria - we can see (yellow circle) that the resolution is estimated to be 40.89 nm.

From the stage evaluations, the two main issues that were addressed were:

1. *Positional error-drifts (FZP/CS Stages)*: evident at system start-up, and would potentially drift hundreds of nanometers (see Figs. 11 & 10) during a scan unless the following corrective/pre-emptive actions are taken:

    1.1. *Active control with interferometry*, actively correct error drifts using interferometric feedback coupled with kinematic models.

    1.2. *System ON/OFF*, optical elements would be positioned after which the stage regulation would be switched off (positioners OFF).

2. *Motion-errors (Sample Stage):* evident during 2D-scans in the XZ-plane. These motion errors, that origi-

ISBN: 978-3-95450-209-7 ISSN: 2226-0358 doi:10.18429/JACoW-ICALEPCS2019-MOCPL06

nated from their respective XZ-stages, were in the order of magnitude of hundreds of nanometers. To circumvent the issue, the following solution was used:

2.1. *Interferometry sample-tracking*, used for image corrections post-process

The resulting 2D- images from Figs. 14 & 15, that used the above-mentioned solutions in points 1.2 & 2.1, further validates the results from the stage evaluations. Furthermore, the utilisation of interferometry is not only found to be useful - but *indispensable* in achieving the 40nm imaging resolution.

Final Words & Project Continuation

Even though not having achieved the 20 nm imaging resolution, the results seem promising with room for progress. The Nanoprobe System, at least in the realm of 2D- sample scans, has therefore been validated at the nanometric level on the SWING beamline. As for project continuation: we will be looking into a better 2D-image resolution, and eventually implementing full 3D-nano-tomo-ptychography.

REFERENCES

[1] C. Engblom *et al.*, "Nanoprobe results: metrology & control in stacked closed-loop systems", in *Proc. ICALEPCS2017*, Barcelona, Spain, Oct 2017, pp. 1028-1033. doi:10.18429/JACoW-ICALEPCS2017-WEAPL04

[2] SWING Beamline at Synchrotron SOLEIL, https://www.synchrotron-soleil.fr/en/beamlines/swing

[3] A. Loulergue *et al.*, "Baseline lattice for the upgrade of SOLEIL", in *Proc. IPAC'18*, Vancouver, BC, Canada, Apr.-May 2018, pp. 4726-4729. doi:10.18429/JACoW-IPAC2018-THPML034

[4] Delta Tau, http://www.deltatau.com

[5] S. Z. Zhang, Y.-M. Abiven, F. Blache, D. Corruble, C. K. Kheffafa, and S. M. Minolli, "Revolution Project: Progress in the Evolution of Soleil Motion Control Model", in *Proc. ICALEPCS'15*, Melbourne, Australia, Oct. 2015, pp. 201–204. doi:10.18429/JACoW-ICALEPCS2015-MOPGF047

[6] Delta Tau MACRO interface, http://www.macro.org/index-1-1.html

[7] Tango Control Systems, https://www.tango-controls.org/

[8] M. Van Heel and M. Schatz, "Fourier shell correlation threshold criteria", in *J. Struct. Biol.*, vol. 151, pp. 250-262, 2005. doi:10.1016/j.jsb.2005.05.009